

The *Arabidopsis* *GTL1* Transcription Factor Regulates Water Use Efficiency and Drought Tolerance by Modulating Stomatal Density via Transrepression of *SDD1*

Chan Yul Yoo,^a Heather E. Pence,^a Jing Bo Jin,^b Kenji Miura,^c Michael J. Gosney,^a Paul M. Hasegawa,^a and Michael V. Mickelbart^{a,1}

^aCenter for Plant Environmental Stress Physiology, Purdue University, West Lafayette, Indiana 47907-2010

^bKey Laboratory of Photosynthesis and Environmental Molecular Physiology, Institute of Botany, Chinese Academy of Sciences, Beijing 100093, China

^cGraduate School of Life and Environmental Sciences, University of Tsukuba, Tsukuba 305-8572, Japan

A goal of modern agriculture is to improve plant drought tolerance and production per amount of water used, referred to as water use efficiency (WUE). Although stomatal density has been linked to WUE, the causal molecular mechanisms have yet to be determined. *Arabidopsis thaliana* *GT-2 LIKE 1* (*GTL1*) loss-of-function mutations result in increased water deficit tolerance and higher integrated WUE by reducing daytime transpiration without a demonstrable reduction in biomass accumulation. *gtl1* plants had higher instantaneous WUE that was attributable to ~25% lower transpiration and stomatal conductance but equivalent CO₂ assimilation. Lower transpiration was associated with higher *STOMATAL DENSITY AND DISTRIBUTION1* (*SDD1*) expression and an ~25% reduction in abaxial stomatal density. *GTL1* expression occurred in abaxial epidermal cells where the protein was localized to the nucleus, and its expression was downregulated by water stress. Chromatin immunoprecipitation analysis indicated that *GTL1* interacts with a region of the *SDD1* promoter that contains a GT3 box. An electrophoretic mobility shift assay was used to determine that the GT3 box is necessary for the interaction between *GTL1* and the *SDD1* promoter. These results establish that *GTL1* negatively regulates WUE by modulating stomatal density via transrepression of *SDD1*.

INTRODUCTION

Drought causes water deficit that limits plant growth and survival because root water uptake from the soil is insufficient to meet the transpirational requirements of the plant (Blum, 1996). Water deficit reduces leaf cell turgor, restricting cell expansion, canopy area development, and photosynthetic source size, thus negatively affecting biomass accumulation and yield (Chaves et al., 2003). An effective plant drought acclimation or adaptation strategy is used to reduce transpirational water loss, which conserves soil moisture and allows plants to maintain an adequate water status to sustain critical physiological and biochemical processes (Nobel, 1999; Chaves et al., 2003). However, a reduction in transpirational water loss often leads to a decline in biomass accumulation because carbon assimilation is also reduced (Sinclair et al., 1984; Udayakumar et al., 1998).

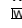
Transpiration and CO₂ uptake occur primarily through stomata, the pores bordered by a pair of guard cells (Hetherington

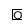
and Woodward, 2003). Conductance through these pores regulates transpirational flux and water use (Bacon, 2004; Chaerle et al., 2005; Morison et al., 2008; Huang et al., 2009; Song and Matsuoka, 2009) and is modulated by stomatal movements (opening and closing) and/or density (Hetherington and Woodward, 2003; Yoo et al., 2009; Casson and Hetherington, 2010; Kim et al., 2010). Alteration of stomatal aperture in response to the environment is a well-understood process that has been linked functionally to drought tolerance and water use efficiency (WUE; Chaerle et al., 2005; Nilson and Assmann, 2007; Kim et al., 2010). Likewise, there is substantial understanding of stomatal development determinants (Bergmann and Sack, 2007; Casson and Hetherington, 2010), and it is known that stomatal density is regulated by environmental factors such as light, CO₂, temperature, humidity, and drought (Lake et al., 2001; Bergmann, 2004; Casson and Gray, 2008; Casson and Hetherington, 2010). However, it is unclear how these environmental factors regulate the developmental determinants and what the consequences of altered stomatal density are on drought tolerance and WUE.

Stomata develop predominantly in the leaf epidermis but do exist in other organs (Bergmann and Sack, 2007; Dong and Bergmann, 2010). Asymmetric division of a protodermal meristemoid mother cell forms a meristemoid and a larger stomatal lineage ground cell, which differentiates into an epidermal pavement cell or another meristemoid. The triangular-shaped meristemoid differentiates into a guard mother cell (GMC) that

¹ Address correspondence to mickelbart@purdue.edu.

The author responsible for distribution of materials integral to the findings presented in this article in accordance with the policy described in the instructions for Authors (www.plantcell.org) is: Michael V. Mickelbart (mickelbart@purdue.edu).

 Online version contains Web-only data.

 Open Access articles can be viewed online without a subscription. www.plantcell.org/cgi/doi/10.1105/tpc.110.078691

undergoes a symmetric division, forming a pair of guard cells. Then, morphogenesis of the stoma occurs (Bergmann and Sack, 2007; Dong and Bergmann, 2010). This basal pathway of stomatal lineage is regulated by well-characterized genetic determinants. *BREAKING OF ASYMMETRY IN THE STOMATAL LINEAGE* and *SPEECHLESS (SPCH)* are necessary for asymmetric division of a meristemoid mother cell to produce a meristemoid (MacAlister et al., 2007; Dong et al., 2009). *MUTE* facilitates meristemoid differentiation to a GMC (MacAlister et al., 2007; Pillitteri et al., 2007). *FAMA* then regulates differentiation of guard cells (Ohashi-Ito and Bergmann, 2006). *INDUCER OF CBF EXPRESSION* (also annotated as *SCREAM*) 1 and 2 physically interact with *SPCH*, *MUTE*, and *FAMA* and regulate the basal pathway (Kanaoka et al., 2008).

A current model for *Arabidopsis thaliana* stomatal development includes a signaling pathway that negatively regulates the basal pathway of stomatal lineage, which is necessary to achieve a balance between pavement and guard cells in the leaf epidermis (Bergmann and Sack, 2007; Casson and Hetherington, 2010). Determinants of this negative signal regulatory pathway include the leucine-rich repeat receptor-like protein *TOO MANY MOUTHS (TMM)* that is presumed to interact with the *ERECTA (ER)* family members of leucine-rich repeat receptor-like kinases (Shpak et al., 2005). *STOMATAL DENSITY AND DISTRIBUTION1 (SDD1)* encodes a subtilisin-like Ser protease that likely processes propeptides into ligands that activate the TMM-ER complex (Berger and Altmann, 2000; von Groll et al., 2002). Ligand interaction with the receptor is presumed to activate a mitogen-activated protein kinase (MAPK) cascade that includes *YODA (YDA; MAPKKK)*, *MKK4/5 (MAPKK)*, and *MPK3/6 (MAPK)*. Then, *SPCH* is phosphorylated by *MPK3/6*, which leads to its inactivation and repression of the basal pathway (Bergmann et al., 2004; Wang et al., 2007; Lampard et al., 2008). Recently, the secretory peptides *EPIDERMAL PATTERNING FACTOR1 (EPF1)*, *EPF2*, and *EPF-like 9* (also annotated as *STOMAGEN*) have been implicated as ligands of TMM that regulate the MAPK cascade, independently of *SDD1* (Hara et al., 2007; Hunt and Gray, 2009; Hunt et al., 2010; Sugano et al., 2010).

The GT-2 transcription factor family proteins contain two trihelix DNA binding domains that interact with GT *cis*-acting elements (GT elements) during transcriptional regulation (Zhou, 1999). GT elements were identified initially in the promoters of light-regulated genes, such as pea (*Pisum sativum*) *RIBULOSE-1,5-BISPHOSPHATE CARBOXYLASE/OXYGENASE SMALL SUBUNIT 3A* and rice (*Oryza sativa*) *PHYTOCHROME A (PHYA)* (Green et al., 1987; Dehesh et al., 1990; Zhou, 1999). GT-2 transcription factor proteins have been implicated in other processes, including endoreduplication, petal development, and abiotic stress tolerance in *Arabidopsis* and soybean (*Glycine max*; Brewer et al., 2004; Breuer et al., 2009; Xie et al., 2009). In this report, evidence is presented that GT-2 LIKE 1 (*GTL1*) functions as a focal regulator of water stress tolerance and WUE through a mechanism that involves transcriptional repression of *SDD1* and regulation of stomatal density and transpiration. *GTL1* expression is downregulated by dehydration, establishing a potential paradigm for how the environment influences stomatal development to reduce transpiration under low water availability conditions.

RESULTS

GTL1 Is Involved in Plant Water Stress Responses

Two independent alleles harboring T-DNA insertions in the first exon and first intron of *Arabidopsis* *GTL1* were annotated as *gtl1-4* (SALK_005972) and *gtl1-5* (SALK_044308) (Figure 1A), respectively, because three other T-DNA insertion alleles (*gtl1-1*, *gtl1-2*, and *gtl1-3*) were described previously (Breuer et al., 2009). The *gtl1-4* T-DNA insertion location is the same as *gtl1-3*, based on sequence data analysis (<http://signal.salk.edu>; Salk Institute Genomic Analysis Laboratory). Homozygous *gtl1-4* and *gtl1-5* plants were identified by PCR amplification using allele-specific primers (Figure 1B; see Supplemental Table 1 online). *GTL1* transcript was undetectable in *gtl1-4* plants but could be detected at very low abundance in *gtl1-5* plants relative to the wild type, which suggests that these mutations may cause loss of function and reduced function of *GTL1*, respectively (Figure 1C).

gtl1-4 and *gtl1-5* plants were better able to survive low relative soil water content (SWC) than were wild-type plants (Figure 1D). More than 80% of *gtl1-4* and *gtl1-5* and <10% of wild-type plants survived SWC of 15% \pm 1.4% (Figure 1E). Most of the wild-type plants wilted at 15% \pm 1.4% SWC, while most *gtl1-4* and *gtl1-5* plants exhibited less severe leaf wilting symptoms (see Supplemental Figure 1A online). Increased water deficit survival of *gtl1* plants was associated with the capacity to maintain higher leaf relative water content (RWC) than the wild type at 13% \pm 1.0% SWC (Figure 1F).

GTL1 transcript was abundant in whole shoots of well-watered 4-week-old Columbia-0 (Col-0) plants but was less abundant in those of plants exposed to water deficit stress caused by withholding irrigation for 11 d (see Supplemental Figure 2A online). This treatment induced expression of the dehydration-responsive *COR15a* gene (see Supplemental Figure 2A online; Baker et al., 1994), indicating the plants were experiencing water deficit. Dehydration stress of detached shoots also caused a reduction in *GTL1* expression (see Supplemental Figure 2B online). Results deposited in the Genevestigator database (<https://www.genevestigator.com>; Zimmermann et al., 2004; Perera et al., 2008) also indicate that *GTL1* is downregulated in response to water deficit stress and was confirmed by the induction of *DREB2A* expression (see Supplemental Figure 2C online; Liu et al., 1998). These results indicate that *GTL1* is expressed when plants have sufficient available water but is downregulated by water deficit.

gtl1 Mutations Improve WUE by Reducing Transpiration

To understand the physiological mechanisms by which *gtl1* plants are more water stress tolerant through maintenance of higher leaf water status under low soil moisture conditions, transpiration rates were assessed by gravimetric analyses over diurnal light/dark periods. *gtl1* plants exhibited lower light period (but not dark period) transpiration rates than wild-type plants when grown under both water-sufficient (Figure 2A) and water deficit (see Supplemental Figure 3 online) conditions. Lower transpiration rates resulted in reduced daily water loss from *gtl1* plants (Figure 2B), which likely enhanced the capacity of *gtl1*

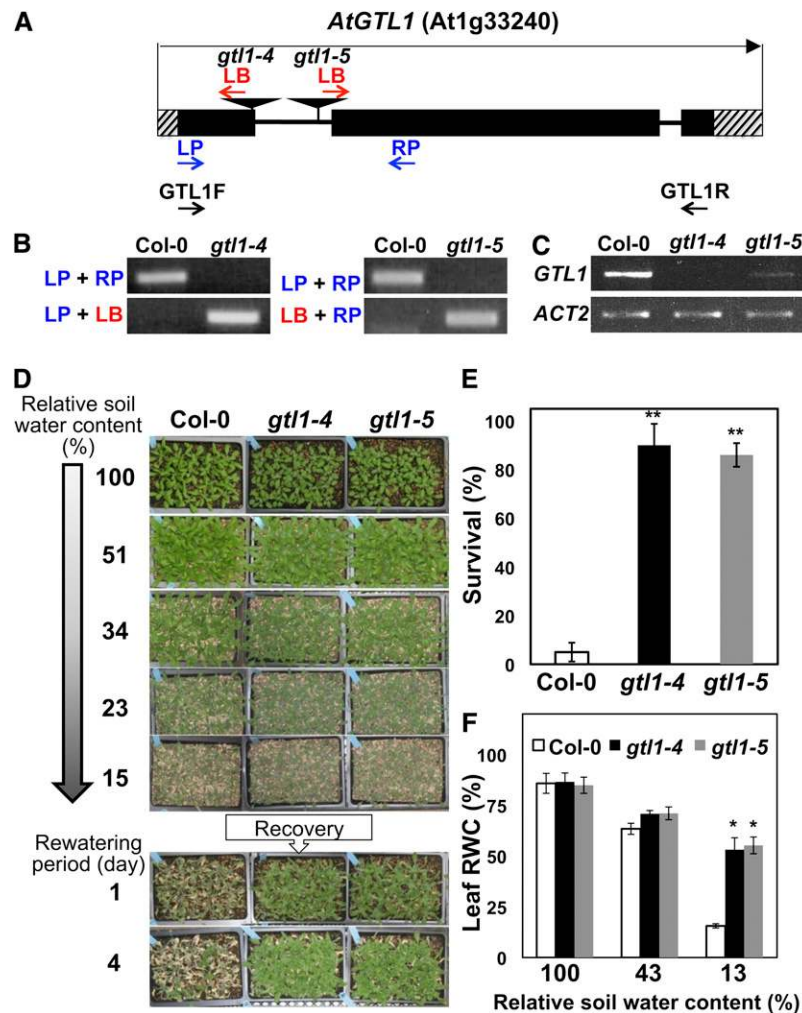


Figure 1. *gtl1* T-DNA Insertional Mutations Enhance Survival and Maintenance of Leaf RWC under Water Deficit Stress.

(A) The schematic illustrates T-DNA locations in the first exon (black bar) and the first intron (black line) in *GTL1* for *gtl1-4* and *gtl1-5*, respectively. Hatched bars indicate 5'- and 3'-untranslated regions. Arrows indicate the positions of primers used in **(B)**.

(B) Homozygosity of the T-DNA insertion in *gtl1-4* and *gtl1-5* was determined by PCR analysis of the *GTL1* genomic fragment using left primers (LP) and right primers (RP) and the T-DNA insertion using a T-DNA-specific left border primer (LB) with LP for *gtl1-4* and LB with RP for *gtl1-5*. Col-0 is the wild type.

(C) *GTL1* expression level in wild-type, *gtl1-4*, and *gtl1-5* plants was determined by RT-PCR analysis with forward and reverse primers (GTL1F and GTL1R) and *ACTIN2* (*ACT2*; reference standard).

(D) and **(E)** Plant water stress responses were analyzed in 3-week-old wild-type and *gtl1* (*gtl1-4* and *gtl1-5*) plants grown under a long-day photoperiod (16 h light/8 h dark, 30% relative humidity). Five containers of each genotype (20 plants/container) were evaluated in three independent experiments. Relative SWC is the soil water relative to the soil water at day 0 of withholding water and is the average of five containers (see Supplemental Figure 1B online). The photograph in **(D)** illustrates results of one replicate from one experiment. Plant survival **(E)** was determined 4 d after rewatering (mean \pm SE, $n = 5$).

(F) In a separate experiment, 4-week-old wild-type and *gtl1* plants were grown under a short-day photoperiod (8 h light/16 h dark, 60% relative humidity) and exposed to water deficit stress by withholding water. Leaf RWC (mean \pm SE, $n = 3$ to 4) and relative SWC (see Supplemental Figure 1C online) were determined. In **(E)** and **(F)**, mean values of *gtl1-4* and *gtl1-5* plants are significantly different from the wild type at * $P < 0.05$ and ** $P < 0.01$.

plants to maintain higher leaf RWC (Figure 1F) and tolerate water deficit stress (Figures 1D and 1E). The significant reduction in transpiration (Figures 2A and 2B) was not associated with decreased shoot dry weight (Figure 2C) or total leaf area (see Supplemental Figures 4A and 4B online), suggesting that re-

duced stomatal conductance, which led to reduced water loss, did not result in a concomitant reduction in biomass accumulation. Consequently, *gtl1* plants had higher integrated WUE (biomass/water use) than did the wild type (Figure 2D). These results indicate that *GTL1* is a negative regulator of WUE.

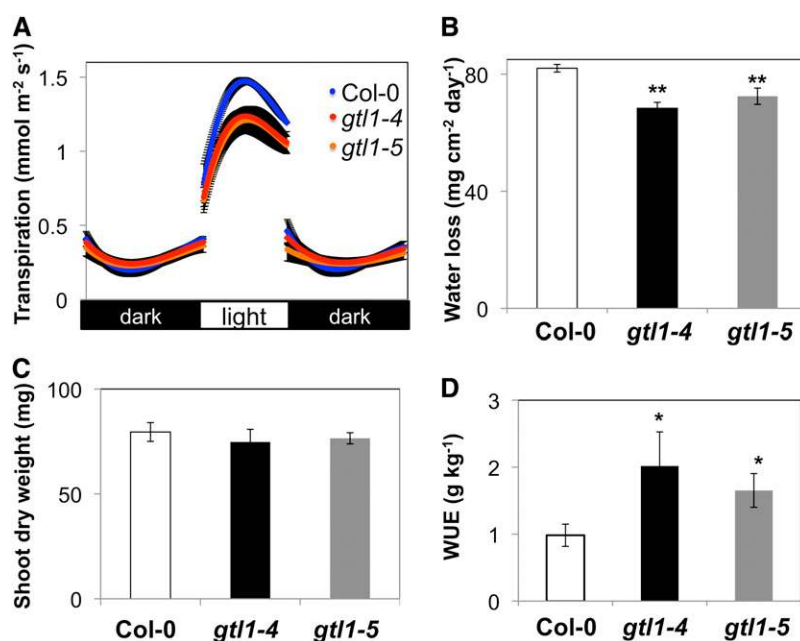


Figure 2. *gtl1* Plants Have Reduced Transpiration and Improved Integrated WUE.

(A) to (C) Diurnal transpiration rate (A) and light period water loss (B) of 5-week-old wild-type (Col-0) and *gtl1* plants grown under a 10-h diurnal photoperiod was gravimetrically determined (mean \pm SE, $n = 4$). Shoot dry weight (C) was measured at the completion of the experiment (mean \pm SE, $n = 4$).

(D) Integrated WUE of wild-type and *gtl1* plants under water-sufficient conditions was calculated from gravimetric measurements of water loss and shoot dry weight over a period of 6 weeks (mean \pm SE, $n = 12$ to 16). In (B) to (D), asterisks indicate that mean values of *gtl1* plants are significantly different from the wild type at * $P < 0.05$ or ** $P < 0.01$.

To test the hypothesis that *gtl1* mutations reduced transpiration to a greater extent than CO₂ assimilation, gas exchange (water and CO₂) of fully expanded leaves of wild-type and *gtl1* plants was determined using an infrared gas analyzer. Leaf transpiration of *gtl1* plants was 26.0% \pm 1.9% lower than that of wild-type plants at saturating light levels (Figure 3A). Stomatal conductance of *gtl1* plants was also lower than in the wild type (Figure 3B), indicating that the reduced transpiration of *gtl1* plants was due to decreased water loss through stomata. Net CO₂ assimilation rates of *gtl1* plants and the wild type were not significantly different (Figure 3C). Consequently, *gtl1* plants had higher instantaneous WUE (CO₂ assimilation/transpiration) (Figure 3D), which was attributable to reduced transpiration (Figure 3A). Vapor pressure deficit (VPD) was similar for all measurements (Figure 3F), indicating that the lower transpiration and stomatal conductance in *gtl1* plants were not due to different VPD.

Quantum efficiency of *gtl1* and wild-type plants was similar (see Supplemental Figure 5A online), indicating there was no difference in the capacity to use photons to fix carbon. In addition, dark respiration and the light compensation point (light intensity at which CO₂ assimilation is equal to respiration) of *gtl1* plants and the wild type were similar (see Supplemental Figures 5B and 5C online). Internal CO₂ concentration (c_i) in leaves of *gtl1* plants was lower than in those of the wild type (Figure 3E), possibly due to a reduced CO₂ flux from the air to the substomatal cavity because of the lower stomatal conductance in *gtl1*

plants. These results indicate that *gtl1* and wild-type plants have equivalent CO₂ assimilation and respiration rates. Furthermore, *gtl1* plants have higher instantaneous WUE, due primarily to reduced transpiration without an appreciable reduction in net CO₂ assimilation and biomass accumulation under our experimental conditions.

GTL1 Regulates Stomatal Density but Does Not Affect Stomatal Aperture or Opening/Closing

gtl1 mutations reduced leaf transpiration because of decreased stomatal conductance (Figures 3A and 3B), which may be caused by effects on stomatal aperture or stomatal density (Hetherington and Woodward, 2003; Yoo et al., 2009). There was no difference in leaf abaxial stomatal aperture of *gtl1* and wild-type plants under water-sufficient conditions (see Supplemental Figure 6A online). Abscisic acid (ABA) treatment caused an equivalent reduction in transpiration rates of *gtl1* and wild-type plants (see Supplemental Figures 6B and 6C online), indicating that both had equivalent stomatal responsiveness to ABA. Seed germination and seedling root growth of *gtl1* plants and the wild type also responded to ABA similarly (see Supplemental Figures 6D and 6E online). These data indicate that GTL1 does not regulate ABA responsiveness, and the lower transpiration rates of *gtl1* plants are not caused by differences in stomatal aperture or ABA-induced stomatal closure.

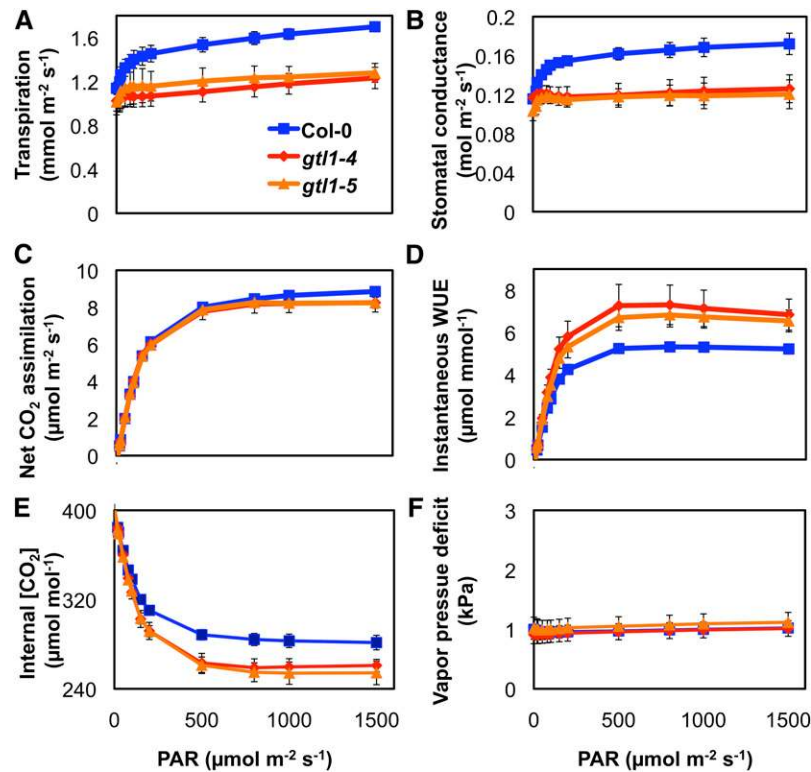


Figure 3. *gtl1* Plants Exhibit Higher Instantaneous WUE Due to Lower Transpiration and Stomatal Conductance.

Leaf transpiration, stomatal conductance, net CO₂ assimilation, instantaneous WUE, internal CO₂ concentration, and VPD were determined on individual leaves of 8-week-old wild-type (Col-0) and *gtl1* plants (8-h diurnal photoperiod) using a Li-Cor 6400 gas exchange system (mean ± SE, *n* = 4).

Fully expanded leaves of *gtl1* plants had fewer stomata than did the wild type (Figure 4), which was determined on the same leaves used for gas exchange analyses (Figure 3). Leaf abaxial stomatal density was $24.1\% \pm 2.5\%$ lower in *gtl1* plants compared with the wild type (Figures 4A and 4B), which correlated with a $26.0\% \pm 1.9\%$ lower transpiration rate at saturating light levels (Figure 3A). The larger leaf trichome phenotype associated with *gtl1* plants (see Supplemental Figure 7 online; Breuer et al., 2009) is unlikely a principal cause of reduced transpiration because any effects on boundary layer conductance due to trichomes would be minimal for small leaves such as those of *Arabidopsis* plants (Jarvis and McNaughton, 1986). These results indicate that higher WUE of *gtl1* plants is due to reduced transpiration that is attributable to a reduction in leaf abaxial stomatal density.

Lower stomatal indices (number of stomata per total number of epidermal cells) caused by *gtl1* (Figure 4C) suggested altered stomatal development in these plants. Stomatal precursor cells, such as meristemoids or GMCs, were detected in leaves of *gtl1* but not wild-type plants (Figures 4A, arrows, and 4D), indicating that stomatal development may be delayed in *gtl1* plants (Bergmann and Sack, 2007; Casson and Hetherington, 2010). Pavement cells were larger in leaves of *gtl1* plants (Figure 4A), which resulted in a lower pavement cell density (Figure 4E). Larger pavement cells in fully expanded leaves of *gtl1* plants may be attributable to unrepressed endoreduplication (Breuer et al., 2009). These results

implicate *GTL1* as a regulator of stomatal and pavement cell development and stomatal density that affects transpiration.

***GTL1* Is Expressed in the Abaxial Epidermis and Negatively Regulates *SDD1* Expression**

Stomatal development genes are expressed primarily in epidermal cells (Bergmann and Sack, 2007; Hunt and Gray, 2009). Analysis of plants transformed with a 2.9-kb *GTL1* promoter- β -glucuronidase (*GUS*) reporter gene fusion (*GTL1_{pro}:GUS*) indicated that the gene is expressed predominantly in guard cells, pavement cells, and meristemoids in the leaf abaxial epidermis (Figures 5A and 5B). *GTL1* localization was determined by monitoring a C-terminal green fluorescence protein (GFP)-tagged fusion protein (*GTL1_{pro}:GTL1:GFP*) (Figure 5C). *GTL1*-GFP expression, which was driven by the same *GTL1* promoter that was used to drive *GUS* expression (Figures 5A and 5B), suppressed the reduced stomatal density phenotype of *gtl1-4* (Figure 5D). The *GTL1*-GFP fusion protein was detected by protein gel blot analysis using anti-GFP (Figure 5E). *GTL1* protein localized to nuclei in abaxial epidermal cells and was detected primarily in pavement cells (Figure 5C). These results indicate that *GTL1* is expressed in guard cells throughout the abaxial epidermis, although *GTL1* accumulates predominantly in pavement cell nuclei.

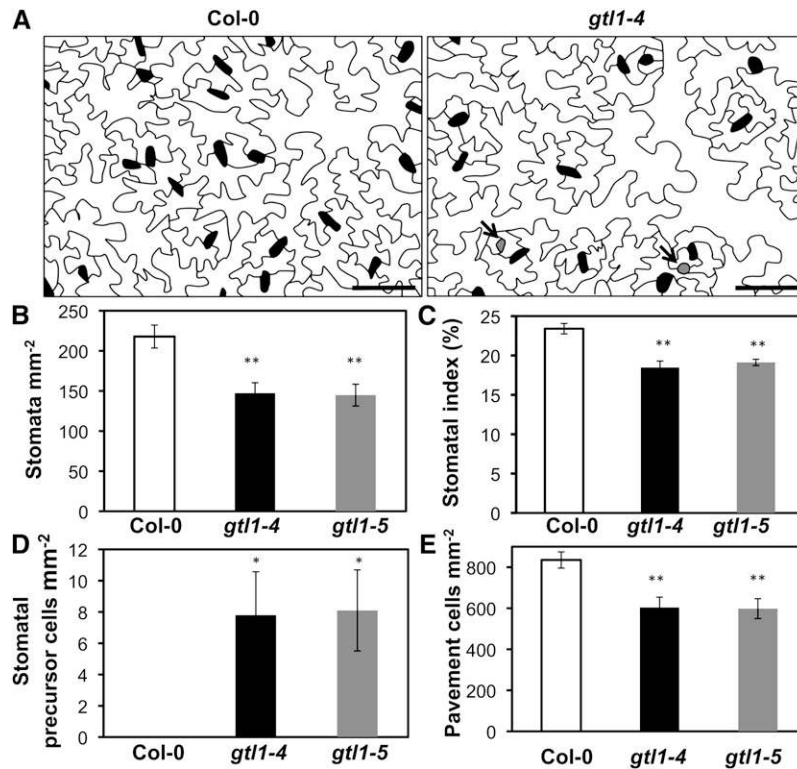


Figure 4. *gtl1* Plants Have Lower Stomatal Densities and Indices and Have Stomatal Precursor Cells.

(A) Representative images of leaf abaxial epidermal layers from 8-week-old wild-type (Col-0) and *gtl1-4* plants (8-h diurnal photoperiod). Pavement cells and stomata are illustrated in white and black, respectively. Stomatal precursor cells (gray) are indicated with arrows. Bars = 50 μ m.

(B) to (E) Stomatal density (the number of stomata per area), stomatal index (the number of stomata per total epidermal cells), the number of stomatal precursor cells, and pavement cell density were analyzed in the leaf abaxial epidermal layers from wild-type and *gtl1-4* plants. Data are the mean of seven individual plants (mean \pm SE, $n = 7$); * and ** indicate significant difference from the wild type at $P < 0.05$ and $P < 0.01$, respectively.

SDD1 activates the MAP kinase pathway that negatively regulates stomatal development (see Supplemental Figure 10 online; Bergmann and Sack, 2007; Casson and Hetherington, 2010). *SDD1* transcript abundance in fully expanded leaves was much higher in *gtl1* compared with wild-type plants (Figure 5F). Similarly, *MPK3* and *MPK6* expression was higher in leaves of *gtl1* plants (Figure 5G). *ER*, *TMM*, and *YDA* expression was similar in *gtl1* and wild-type plants (see Supplemental Figure 8 online). Thus, GTL1 appears to function as a stomatal development determinant by negatively regulating *SDD1*, *MPK3*, and *MPK6* expression.

GTL1 Binds to the GT Element in the *SDD1* Promoter

GT-2 transcription factor family proteins bind to GT elements (GT1 box, GGTTAA; GT2 box, GGTAAT; GT3 box, GGTAAG) in the promoters of target genes to activate or repress transcription (Kuhn et al., 1993; Ni et al., 1996; Zhou, 1999). Initially, GTL1 DNA binding activity was assessed using the rice *PHYA* promoter fragment that has been reported to interact with *Arabidopsis* and rice GT2 proteins (Kuhn et al., 1993; Ni et al., 1996). Two partial fragments of GTL1 (Nt1 and GTL1N polypeptides) were fused with maltose binding protein (MBP) to enhance solubility during

purification (Figure 6A). An electrophoretic mobility shift assay (EMSA) determined that only GTL1N interacted with the rice *PHYA* promoter fragment (Figure 6B). The Nt1 polypeptide that was predicted to have an incomplete DNA binding domain did not interact with the *PHYA* promoter (Figures 6A and 6B). Unlabeled probe was an effective competitor (Figure 6C), indicating that GTL1N specifically binds to the *PHYA* promoter. Furthermore, the GTL1 N-terminal DNA binding domain effectively bound all three types of GT elements (see Supplemental Figure 9 online).

We hypothesized that GTL1 binds directly to the GT3 box (GGTAAA; -428 to -423) of the *SDD1* promoter to repress *SDD1* transcription. Migration of labeled *SDD1* promoter was shifted by the addition of GTL1N polypeptide. However, this gel shift was abolished by adding unlabeled *SDD1* promoter (Figure 6D), indicating that GTL1 specifically binds to the *SDD1* promoter. Two guanine residues in the GT3 box (GGTAAA) are critical nucleotides in the interaction of GT elements with GT2 family proteins (Kuhn et al., 1993; Ni et al., 1996). We substituted CC for GG in the GT3 box (GGTAAA \rightarrow CCTAAA) in the *SDD1* promoter fragment to determine specificity of the GT3 box for GTL1 DNA binding activity. The mutated *SDD1* promoter was used as a noncompetitor (unlabeled mutated *SDD1* promoter)

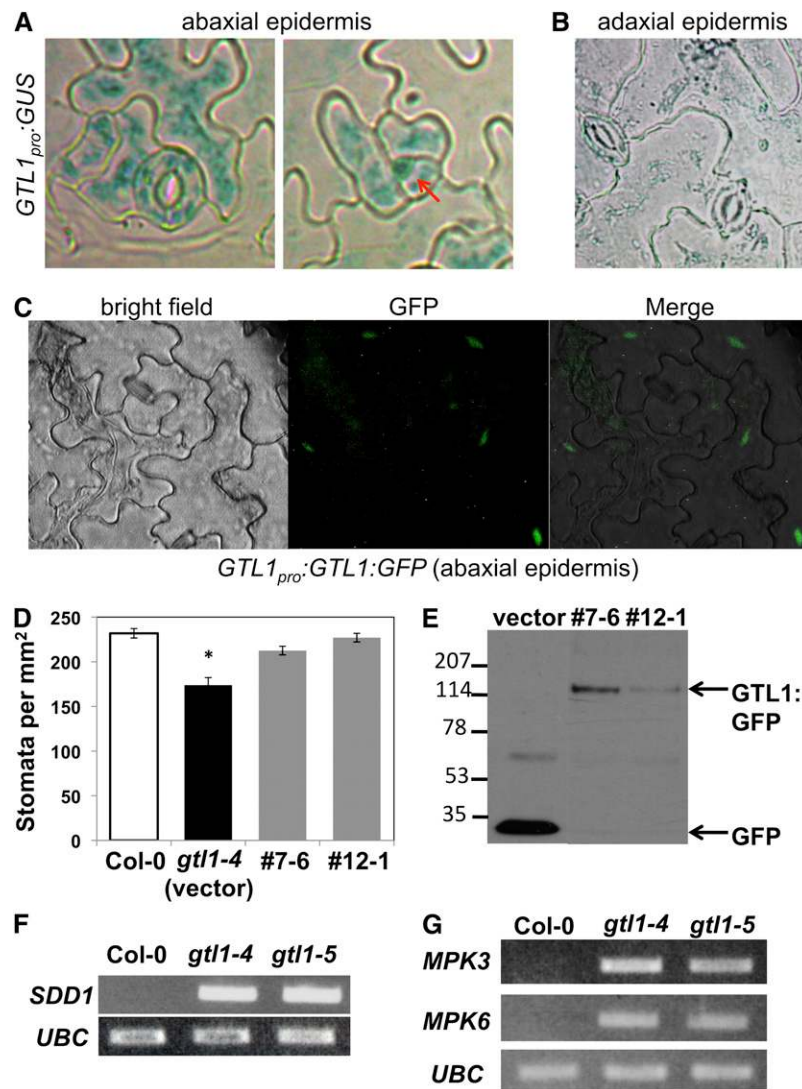


Figure 5. *GTL1* Is Expressed in the Abaxial Epidermis and Negatively Regulates *SDD1* Expression.

(A) GUS activity in the abaxial epidermis of the first rosette leaf from 10-d-old seedlings harboring *GTL1*_{pro}:GUS was analyzed by histochemical staining. Arrow indicates a triangle-shaped meristemoid.
 (B) GUS activity was not detected in the adaxial epidermis of fully expanded rosette leaves from 4-week-old transgenic plants harboring *GTL1*_{pro}:GUS.
 (C) *GTL1*-GFP protein localization was analyzed in the leaf abaxial epidermis of 4-week-old transgenic plants harboring *GTL1*_{pro}:*GTL1*:GFP (#12-1) by fluorescence microscopy.
 (D) Stomatal density was measured in 6-week-old wild-type (Col-0), *gtl1-4* (empty vector control line), and *GTL1*_{pro}:*GTL1*:GFP complementation lines (#7-6 and #12-1) (mean ± SE, *n* = 4; * indicates significant difference from the wild type at *P* < 0.05).
 (E) *GTL1*-GFP protein expression in 6-week-old complementation lines and GFP protein expression in 6-week-old empty vector control plants were detected by immunoblot using anti-GFP antibody.
 (F) and (G) RT-PCR analysis of *SDD1*, *MPK3*, *MPK6*, or *UBC* was performed on total RNA from fully expanded leaves of 8-week-old wild-type and *gtl1* plants.

and did not inhibit the interaction between *GTL1* and the *SDD1* promoter (Figure 6D). Furthermore, *GTL1N* did not bind to the labeled mutated *SDD1* promoter (GG → CC) (Figure 6E). The results of an in vitro EMSA indicate that *GTL1* specifically binds to the GT3 box in the *SDD1* promoter.

In vivo interaction of *GTL1* with the *SDD1* promoter was tested by chromatin immunoprecipitation (ChIP) analysis using trans-

genic plants harboring the *GTL1*_{pro}:*GTL1*:GFP construct that suppressed the reduced stomatal density phenotype of *gtl1-4* plants (Figures 5D and 5E). Chromatin associated with *GTL1*-GFP was immunoprecipitated with anti-GFP antibody and subjected to PCR analysis using primers specific for different regions of the *SDD1* promoter (see Supplemental Table 1 online). Region 3 (−279 to −556) included the GT3 box in the *SDD1* promoter.

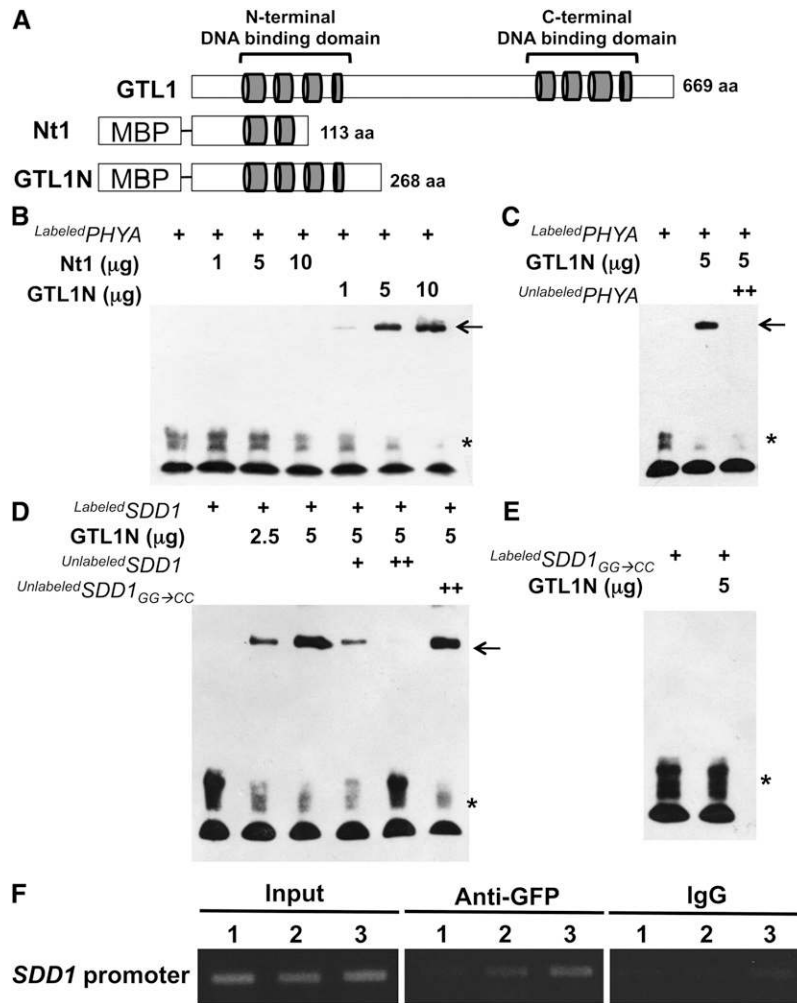


Figure 6. N-Terminal DNA Binding Domain of GTL1 Binds to *PHYA* and *SDD1* Promoters.

(A) Schematic diagram of the GTL1 protein, showing the four helical, N- and C-terminal DNA binding domains (represented as gray cylinders). Two protein fragments (Nt1 and GTL1N) were fused with MBP.

(B) Nt1 and GTL1N polypeptides and a biotin-labeled rice *PHYA* promoter fragment (400 ng) were used for EMSA. In **(B)** to **(E)**, free probe and GTL1N-probe complexes are indicated by an asterisk and arrows, respectively.

(C) Unlabeled *PHYA* promoter (2 μ g) was used as a competitor to determine the specificity of DNA binding activity for GTL1N.

(D) GTL1N polypeptide was used for EMSA with a biotin-labeled *SDD1* promoter fragment (250 ng). Unlabeled probes (250 ng [+], and 1 μ g [++]) were used as competitors. An unlabeled mutant version of the *SDD1* promoter (GG \rightarrow CC) was used as a noncompetitor.

(E) The mutant version of the *SDD1* promoter (GG \rightarrow CC) was labeled with biotin (250 ng) and used for EMSA with GTL1N polypeptides.

(F) ChIP analysis was conducted to determine the *in vivo* interaction between GTL1 with the *SDD1* promoter. Input is chromatin before immunoprecipitation. Anti-GFP antibody was used to precipitate chromatin associated with GTL1-GFP. Mouse IgG was used as a negative control for the specificity of immunoprecipitation. The *SDD1* promoter region associated with GTL1 was amplified by PCR using *SDD1* promoter-specific primers for three different regions (1, 2, and 3). Region 1 (–1136 to –1400) is distal to the GT3 box. Region 2 (–538 to –824) is adjacent to, but does not contain, the GT3 box. Region 3 (–279 to –556) includes the GT3 box in the *SDD1* promoter.

Region 2 (–538 to –824) was adjacent to, but did not contain, the GT3 box. Region 1 (–1136 to –1400) was distal to the GT3 box. Region 3 primers resulted in the greatest amount of PCR product (Figure 6F). The amount of PCR amplification product was reduced with primers for region 2 and even more so with those for region 3 (Figure 6F). These results are consistent with the GTL1 fragment binding to the GT3 box in the *SDD1* promoter determined by *in vitro* DNA binding (Figure 6D). Together, these

results indicate that GTL1 binds to the *SDD1* promoter to repress *SDD1* expression, which regulates stomatal density.

DISCUSSION

The trihelix transcription factor GTL1, previously identified as a trichome development regulator (Breuer et al., 2009), is shown herein to regulate stomatal development. Furthermore, *GTL1*

loss-of-function mutations enhanced water deficit tolerance, which was associated with maintenance of leaf water status, even when plants were grown in media with low SWC (Figure 1). *gtl1* mutations caused higher instantaneous and integrated plant WUE because of reduced transpiration that occurred without a difference in net CO₂ assimilation (Figures 2 and 3). Lower transpiration, drought tolerance, and higher WUE were associated with reduced stomatal density in the leaf abaxial epidermis and higher *SDD1* expression (Figures 4 and 5F), which suggests that *gtl1* reduced stomatal density by increasing expression of *SDD1*, a negative regulator of stomatal development (Berger and Altmann, 2000; von Groll et al., 2002). *GTL1* expression was downregulated by plant water deficit (see Supplemental Figure 2 online), and *GTL1* localized to the nucleus in abaxial epidermal pavement cells (Figure 5C). EMSA indicated that *GTL1* physically interacts with the GT3 box in the *SDD1* promoter, and ChIP analysis confirmed that *GTL1* was associated with the GT3 box of the *SDD1* promoter (Figures 6D and 6F). Together, these results indicate that *GTL1* regulates plant water use by modulating stomatal development through *SDD1* transrepression (Figure 7).

GTL1 Affects Plant Water Use and CO₂ Assimilation through Regulation of Stomatal Development

Transpiration and CO₂ uptake occur primarily through stomatal pores, and conductance is dependent on stomatal density and pore aperture (Hetherington and Woodward, 2003; Nilson and Assmann, 2007). *gtl1* caused a reduction in leaf abaxial surface stomatal density (Figure 4) and decreased transpiration (Figures 2 and 3), which resulted in enhanced water deficit tolerance (Figure 1D). Reduced stomatal density caused by *gtl1* did not

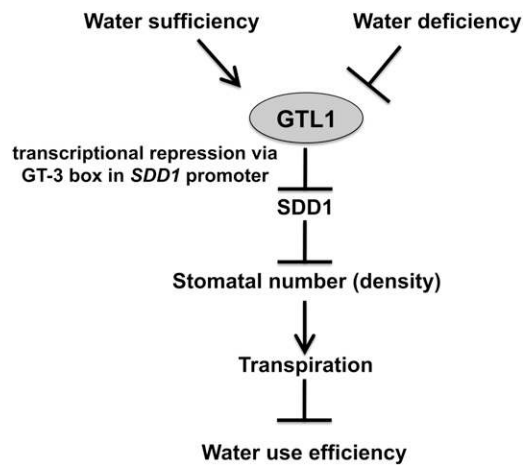


Figure 7. Model of *GTL1* Function as a Determinant of WUE by Regulating Stomatal Density through Transrepression of *SDD1*.

GTL1 binds to the GT element (GT3 box: GGTAAG) in the *SDD1* promoter to transrepress *SDD1*, which is a negative regulator of stomatal development. *GTL1* negatively regulates WUE by positively regulating stomatal density and transpiration through transrepression of *SDD1*. *GTL1* is expressed in water-sufficient conditions to facilitate stomatal development and is downregulated under water deficit to reduce transpiration.

affect CO₂ assimilation and biomass accumulation and resulted in higher integrated and instantaneous plant WUE (Figures 2 to 4). For most C3 plants, net CO₂ assimilation rate saturates as stomatal conductance increases because of nonstomatal limitations, such as the regeneration of ribulose 1,5-bisphosphate (Farquhar and Sharkey, 1982). However, over a similar stomatal conductance range, transpiration will continue to increase linearly with stomatal conductance (Yoo et al., 2009). Therefore, a moderate decrease in stomatal density can reduce transpiration significantly without a concomitant effect on CO₂ assimilation and result in higher WUE (Yoo et al., 2009). It is plausible that a more substantial reduction in stomatal density would reduce CO₂ uptake substantially and lower both WUE and biomass accumulation. Consistent with this hypothesis, cauliflower mosaic virus 35S-driven *SDD1* expression in C24 plants resulted in an ~60% reduction in stomatal density that was linked to a 20% reduction in net CO₂ assimilation rate (Büßis et al., 2006).

Genetic variation for WUE is negatively correlated with transpiration in primary gene pools (Van den Boogaard et al., 1997; Impa et al., 2005; Yoo et al., 2009). *ER*, *GPA1*, *CA1/4*, and *HDG11* are *Arabidopsis* genetic determinants known to regulate WUE through modulation of stomatal density (Masle et al., 2005; Yu et al., 2008; Hu et al., 2010; Nilson and Assmann, 2010). *ER* alleles were the cause of quantitative trait loci associated with natural variation in WUE between Col-4 and Landsberg erecta (Masle et al., 2005). *ER* mutations resulted in lower WUE, which was associated with a number of measurable phenotypes, including increased stomatal density and reduced photosynthetic capacity and mesophyll development (Masle et al., 2005). *GPA1* (G protein α -subunit 1) loss of function resulted in reduced stomatal density and stomatal conductance but similar net CO₂ assimilation leading to higher WUE (Nilson and Assmann, 2010). Improved WUE of *gpa1* plants was due primarily to reduced stomatal density rather than to insensitivity to ABA-induced stomatal closure or to inhibition of stomatal opening (Fan et al., 2008; Nilson and Assmann, 2010). *CA1* and *CA4* (carbonic anhydrase 1 and 4) have also been implicated in the regulation of WUE (Hu et al., 2010). *ca1 ca4* double mutations increased stomatal density, whereas guard cell-targeted overexpression of *CA1* or *CA4* in *ca1 ca4* plants decreased stomatal density and improved WUE (Hu et al., 2010). The target determinants and molecular mechanisms by which *GPA1*, *CA1*, and *CA4* regulate stomatal development and WUE remain to be elucidated.

A forward genetic screen of a T-DNA activation-tagged population for drought tolerance resulted in the identification of *enhanced drought tolerance1* (*edt1*). The T-DNA in *edt1* was inserted in the 5'-untranslated region of *HOMEODOMAIN GLABROUS 11* (*HDG11*) and resulted in overexpression of *HDG11*, reduced stomatal density, and higher WUE. Drought tolerance and higher WUE were attributable to reduced stomatal density and transpiration and to enhanced root growth, photosynthesis, and ABA and Pro biosynthesis (Yu et al., 2008). *ER* expression was greater in *edt1*, and *HDG11* transactivated the *ER* promoter when cotransformed into onion cells, implying that *HDG11* directly activates *ER* expression and may regulate stomatal development through the negative regulatory pathway as does *GTL1*. The recent characterization of these genetic determinants that affect WUE indicates that plants have the capacity to

optimize water use and CO₂ assimilation by regulating stomatal development.

GTL1 Is a Positive Regulator of Stomatal Development as a Transrepressor of *SDD1*

SDD1 and *MPK3/6* transcripts were misupregulated in *gtl1* plants (Figures 5F and 5G), indicating that GTL1 functions upstream of these determinants in the negative regulatory pathway (see Supplemental Figure 10 online; Bergmann and Sack, 2007). GTL1 interacted with the GT3 box in an *SDD1* promoter fragment in vitro (Figure 6D) and was associated with an *SDD1* promoter fragment in chromatin that contained the GT3 box (Figure 6F). These data indicate that GTL1 is a transcriptional repressor of *SDD1* and, through this function, positively regulates stomatal density (see Supplemental Figure 10 online; Bergmann and Sack, 2007; Casson and Hetherington, 2010).

The developmental program that determines stomatal density is sufficiently plastic to enable plants to regulate CO₂ uptake and transpiration in response to changing environments (Casson and Gray, 2008). Climatic factors (e.g., light, CO₂, relative humidity, and water deficit) and hormones alter stomatal density (Lake et al., 2001; Bergmann, 2004; Casson and Gray, 2008; Xu and Zhou, 2008; Ahmed et al., 2010), although the mechanism(s) by which these effectors modulate stomatal development has not been identified (Casson and Hetherington, 2010). *GTL1* transcript was abundant when plants were growing with adequate water supply but expression was downregulated by water stress or dehydration (see Supplemental Figure 1 online). This drought-responsive downregulation of *GTL1* expression may indicate that the transcription factor is an integrative node that links stomatal development to environmental regulation of density and gas exchange (Figure 7). Further investigation is necessary to determine the mechanisms by which other environmental factors regulate stomatal development and to determine the adaptive significance of these as plants cope with climatic fluctuations.

GTL1 was expressed in both pavement and guard cells of the leaf abaxial epidermis, but expression was not detected in the adaxial epidermis (Figures 5A and B), which correlates with *GTL1* regulation of abaxial stomatal density (Figure 4A). *GTL1* accumulated in the nuclei of pavement cells (Figure 4C), where *SDD1* is not expressed (von Groll et al., 2002), which is consistent with the notion that *GTL1* transrepresses this negative regulator of stomatal development. These *GTL1* expression and protein localization data, together with high expression of *SDD1* in *gtl1* plants, indicate that *SDD1* repression by GTL1 is necessary to allow formation of stomata during development and, in response to environmental changes, to optimize transpiration and CO₂ assimilation. Further research is needed to determine whether tissue- and cell type-specific regulation of *SDD1* is mediated by GTL1 and environmental changes.

GTL1 Fine-Tunes Stomatal Development to Regulate WUE

ER and TMM are known receptors of the signal cascade that negatively regulates the basal stomatal development pathway (see Supplemental Figure 10 online; Shpak et al., 2005; Bergmann and Sack, 2007). *SDD1* encodes a subtilisin-like protease that

activates ER and TMM to repress stomatal development (von Groll et al., 2002; Shpak et al., 2005). These receptors are negatively regulated by *EPF1/2* ligands and positively regulated by *STOMAGEN*, independent of *SDD1* (von Groll et al., 2002; Hara et al., 2007; Hunt and Gray, 2009; Sugano et al., 2010). It is plausible that convergent functions of *EPF1/2*, *STOMAGEN*, and *SDD1* on ER and TMM receptors are necessary for precise regulation of stomatal number and plant water use in different ecosystems and in response to developmental and environmental cues (Casson and Hetherington, 2010). We posit that GTL1 is a determinant that integrates the effects of plant water-deficit stress on stomatal development to regulate carbon assimilation and transpiration. It is possible that other members of the GT-2 family that are closely related to GTL1 may have similar functions as transcriptional repressors of *SDD1* expression. The existence of multiple regulatory determinants to optimize gas exchange and improve WUE in different environments is analogous to fine-tuning of signal transduction that is necessary for amplification and/or maintenance of a signal and for reducing noise fluctuations of signals (Thattai and van Oudenaarden, 2001; Kashiwagi et al., 2006; Saez et al., 2006; Alon, 2007).

METHODS

Plant Materials and Growth Conditions

Arabidopsis thaliana genetic resources were wild type (Col-0 ecotype), *gtl1-4* (SALK_005972), and *gtl1-5* (SALK_044308). *gtl1* mutant seeds were obtained from the ABRC at Ohio State University. Transgenic plants harboring and expressing *GTL1_{pro}:GUS* and *GTL1_{pro}:GTL1:GFP* were generated using the *Agrobacterium tumefaciens*-mediated floral dip method (Zhang et al., 2006). Single-copy and homozygous T3 plants were identified by genetic segregation on agar medium containing hygromycin. Seeds were stratified for 3 d at 4°C in the dark and then sown onto medium (1× Murashige and Skoog basal salt mixture, 2% sucrose, 2.5 mM MES, pH 5.7, and 0.8% agar) or in a 2:1 mixture of ProMix PGX soilless media (Premier Horticulture) and Turface calcined clay (Profile Products) in containers (200 mL, 1 liter, or 1.7 liter) or Falcon tubes (50 mL). Plants grown on agar were maintained in a growth room (temperature: 22°C [light]/18°C [dark]; photoperiod: 16 h [light]/8 h [dark]; light intensity: ~80 μmol quanta m⁻² s⁻¹; provided by fluorescent bulbs). Plants grown in soilless media were maintained in a controlled environment growth chamber (temperature: 22°C [light]/18°C [dark]; light intensity: ~125 μmol quanta m⁻² s⁻¹ provided by fluorescent bulbs; relative humidity: ~60%). Photoperiods for soilless media-grown plants are described in the corresponding figure legends.

Plasmid Construction

GTL1 promoter (*GTL1_{pro}*):GUS was constructed in the pCambia1303 vector (Cambia). The 2973-bp *GTL1* promoter was amplified by designated primers (GTL1p-F-XmaI and GTL1p-R-NcoI) (see Supplemental Table 1 online). After the 35S promoter in pCambia1303 was removed by *XmaI* and *NcoI* digestion, the *GTL1* promoter was inserted to the *XmaI*/*NcoI* site. For *GTL1_{pro}:GTL1:GFP* construction, the open reading frame of *GTL1* was amplified by designated primers (GTL1-F-XmaI and GTL1-R-SpeI) from cDNA. The amplified *GTL1* open reading frame was inserted into the *XmaI* and *SpeI* sites in the pCambia1302 vector (Cambia) after the 35S promoter was removed and was fused to GFP in frame (pCambia1302-GTL1:GFP). Then, the *GTL1* promoter, amplified by designated primers (GTL1p-F-XmaI and GTL1p-R-XmaI), was inserted

into the *Xma*I site in *pCAMBIA1302-GTL1:GFP*. *MBP:GTL1* was constructed in the pMAL-C2 vector (Kim et al., 2007). Two *GTL1* fragments (Nt1 and *GTL1N*) were amplified by designated primers (Nt1, Nt1-F-EcoRI and Nt1-R-PstI; *GTL1N*, Nt1-F-EcoRI and Nt2-R-PstI). The two amplified fragments were inserted into the *Eco*RI and *Pst*I sites in the pMAL-C2 vector. Sequence information for all designated primers used for plasmid construction is provided in Supplemental Table 1 online.

Physiological Analyses

Water deficit stress was imposed by withholding water from containers (1 liter) with 288.7 ± 3.1 g (dry weight) of soilless media containing 20 plants (3 weeks old). Containers were irrigated with water to saturation and weighed at the start of water deficit stress treatment (initial weight) and then periodically throughout the treatment period. Relative SWC was calculated as (final fresh weight – dry weight)/(initial weight – dry weight) $\times 100$. After 14 d, plants were rewatered and survival was assessed 4 d after rewatering. In a separate experiment, leaf RWC of fully expanded leaves from 4-week-old plants grown in 200-mL containers at different relative SWC was assessed. Leaves were removed and immediately weighed to obtain leaf FW. Leaves were then placed into vials filled with distilled water for 24 h, blotted to remove excess water, and then weighed to obtain leaf turgid weight (TW). Leaves were then dried to a constant weight at 65°C and reweighed to obtain leaf dry weight (DW). Leaf RWC was calculated as $(FW - DW)/(TW - DW) \times 100$.

Whole-plant transpiration of 5- to 6-week-old plants was determined by a gravimetric method. Individual plants were grown in 200-mL containers. During the period that transpiration was measured, each container was covered with a polyethylene wrap to prevent evaporation from the soil surface. An individual plant was placed onto a balance, and the weight of each container was determined every 5 min. At the end of the experiment, total leaf area was determined from photographs of excised leaves using the ImageJ program (National Institutes of Health). Transpiration rate ($\text{mmol water m}^{-2} \text{ s}^{-1}$) was calculated based on gravimetric water loss rate and leaf area data. A curve was fit to the data using a 12-point moving average. A cubic polynomial was then fit to the smoothed data separately for the day period. The equation for the light period transpiration curve was then differentiated and solved for zero to give the time at which maximum transpiration occurs. This time was then used to calculate maximum light period transpiration rate.

Integrated WUE was calculated as final shoot dry weight divided by total water loss over a period of 6 weeks. Individual containers were covered with plastic wrap containing a central hole through which three to four seeds for each genotype were sown. Seven days after germination, containers were thinned to one seedling per container. Individual containers were weighed before and after irrigating with water every 5 to 6 d to determine moisture loss. Water loss from control containers (without plants) was subtracted from treatment containers. Shoot dry weight was determined at the end of the experiment.

Leaf gas exchange of fully expanded leaves, including transpiration, stomatal conductance, and net CO_2 assimilation, was determined using a LI6400XT infrared gas analyzer (LI-COR Biosciences). Plants were grown for 60 d in 1.7-liter containers under short-day conditions (8 h light). These conditions resulted in plants with leaves large enough to fill the 6-cm² LI-6400 chamber. Gas exchange was measured at PAR levels of 1500, 1000, 800, 500, 200, 150, 100, 80, 50, 25, 20, and 0 $\mu\text{mol m}^{-2} \text{ s}^{-1}$. A nonrectangular hyperbola curve was fit to the net CO_2 assimilation data (Lambers et al., 1998). Quantum efficiency is the initial slope of the curve, dark respiration is the point at which the curve crosses the y axis at PAR = 0, and the light compensation point is the point at which the curve crosses the x axis (Lambers et al., 1998). VPD during measurement was ~ 1 kPa. Instantaneous WUE was calculated as net CO_2 assimilation rates divided by transpiration rates.

Anatomical Analysis

Abaxial epidermal anatomy of fully expanded leaves from plants that were used for leaf gas exchange analyses was characterized. Transparent cellulose adhesive tape was attached to the middle portion of the adaxial lamina, and mesophyll layers of the leaf were removed by pulling the tape so that only the abaxial epidermis remained. The abaxial epidermis was placed on a slide and images were obtained under $\times 200$ magnification using a Nikon-OptiPhot2 microscope. Stomatal density (stomatal number per area), stomatal index (ratio of stomata to total epidermal cells, including stomata, stomatal precursor cells, and pavement cells), the number of stomatal precursor cells, and pavement cell density (pavement cells per area) were obtained from a leaf area of 0.069 mm². In all calculations, stomata were considered to be a pair of guard cells. Stomatal precursor cells were identified as cells at the meristemoid or GMC stage. These were not counted as stomata. The OminiGraffle Pro program was used to transform microscopy images to simplified black and white images.

Stomatal aperture was analyzed in abaxial epidermal peels from fully expanded leaves (Li et al., 2006). The epidermis was incubated in buffer solution (20 mM KCl, 5 mM MES-KOH, and 1 mM CaCl_2 , pH 6.15) under $\sim 200 \mu\text{mol m}^{-2} \text{ s}^{-1}$ for 4 h. Subsequently, the epidermis was placed onto a slide and images were photographed using a Nikon-OptiPhot2 microscope ($\times 400$ magnification). The aperture width of each stomatal pore was determined from the image.

Histochemical Assay for GUS Activity

Epidermal peels from T3 transgenic plants harboring *GTL1_{pro}:GUS* were incubated in a fixation solution (0.3% formaldehyde, 10 mM MES, pH 5.6, and 0.3 M mannitol) for 1 h, washed with 50 mM sodium phosphate buffer, and then incubated further in staining solution (50 mM sodium phosphate buffer, 2.5 mM potassium ferricyanide, 2.5 mM potassium ferrocyanide, 0.3% Triton X-100, and 1.9 mM 5-bromo-4-chloro-3-indolyl β -D-glucuronide) for 12 h at 37°C. Tissues were then washed several times in 70% ethanol until chlorophyll was completely extracted.

Fluorescence Microscopy for GFP Imaging

Subcellular localization of *GTL1-GFP* fusion protein in the abaxial epidermis of 4-week-old transgenic plants harboring *GTL1_{pro}:GTL1:GFP* was determined. A Nikon-OptiPhot2 microscope with epifluorescence was used to detect GFP expression using a B1E filter (excitation 470 to 490 nm; dichroic mirror 515 nm; barrier filter 520 to 560 nm). Images were photographed with a digital camera.

Purification of MBP-GTL1 Fusion Proteins

MBP-GTL1 fusion protein was expressed in BL21 *Escherichia coli* cells after induction with 0.1 mM of isopropyl β -D-thiogalactopyranoside and incubation for 2 h at 30°C. The culture was harvested by centrifugation for 5 min at 5000g. The pellet was resuspended in 50 mL of ice-cold MBP resuspension buffer (10 mM Tris-Cl, pH 7.5, 30 mM NaCl, 1 mM EDTA, 1 mM PMSF, and 1 \times Protease inhibitor cocktail), sonicated with a 550 Sonic Dismembrator (Fisher Scientific), and then centrifuged for 20 min at 14,000g. The supernatant was incubated with prewashed amylose resin (NEB) for 2 h at 4°C and washed five times with buffer (10 mM Tris-Cl, pH 7.5, and 1 M NaCl). MBP-GTL1 protein was eluted with buffer (10 mM Tris-Cl, pH 7.5, and 10 mM maltose). The eluate was collected with a centrifugal filter (Amicon Ultra 50K; Millipore) for buffer exchange according to the manufacturer's protocol. The fusion protein was suspended in buffer (100 mM potassium phosphate, pH 7.8, 1 mM EDTA, 1% Triton X-100, and 10% glycerol).

EMSA

MBP-GTL1 fusion proteins purified on amylose resin were used to determine DNA binding by EMSA. Single-stranded complementary oligonucleotide fragments corresponding to regions of *Arabidopsis SDD1* or rice (*Oryza sativa*) *PHYA* promoters (see Supplemental Table 1 online) that included the GT elements were synthesized (Macrogen) and biotinylated using the Biotin 3'-end DNA labeling kit (Thermo Fisher Scientific). Biotinylated complementary oligonucleotide pairs were annealed to make double-stranded and biotin-labeled probes (100 ng μL^{-1}) by mixing in a buffer (10 mM Tris and 1 mM EDTA), boiling for 5 min, and cooling slowly overnight. Unlabeled complementary oligonucleotide pairs were also annealed to make double-stranded competitor probes (500 ng μL^{-1}). EMSA reaction solutions were prepared by adding the following components in order according to the manufacturer's protocol (LightShift Chemiluminescent EMSA kit; Thermo Fisher Scientific): 1 \times binding buffer, 50 ng poly (dI-dC), 2.5% glycerol, 0.06% Nonidet P-40, 5 mM MgCl_2 , 19 μg BSA, proteins, competitor, noncompetitor, and biotin-labeled probes. Reaction solutions were incubated for 20 min at room temperature. The protein-probes mixture was separated in a 6% polyacrylamide native gel and transferred to a Biotinylated Nylon membrane (Thermo Fisher Scientific). Migration of biotin-labeled probes was detected on x-ray film using streptavidin-horseradish peroxidase conjugates that bind to biotin and chemiluminescent substrate according to the manufacturer's protocol.

ChIP Assay

Leaves of 3-week-old T3 transgenic plants harboring *GTL1pro::GTP1::GFP* were used for ChIP analysis. Anti-GFP antibody was used to pull down the chromatin, as described previously (Jin et al., 2008). Leaves were incubated in buffer (0.4 M sucrose, 10 mM Tris, pH 8.0, 1 mM EDTA, 1 mM PMSF, and 1% formaldehyde) under vacuum for 15 min to cross-link the chromatin. Then, 0.1 M Gly was added to the mixture, which was incubated for an additional 5 min to terminate the reaction. Leaves were ground in liquid nitrogen and resuspended in lysis buffer (50 mM HEPES, pH 7.5, 150 mM NaCl, 1 mM EDTA, 1% Triton X-100, 0.1% deoxycholate, 0.1% SDS, 1 mM PMSF, 10 mM Na-butyrate, and 1 \times complete protease inhibitor [Roche]). Chromatin was sheared to ~200- to 1000-bp fragments by sonication and then centrifuged. Supernatants were precleared with protein G/salmon sperm DNA (protein G agarose beads) for 1 h at 4°C. After centrifugation, supernatant including chromatin (input material) was used for immunoprecipitation with anti-GFP antibody (Santa Cruz Biotechnology) or mouse IgG antibody (Abcam). Anti-GFP antibody bound to GTL-GFP-chromatin complexes was incubated with protein G agarose beads for 1 h at 4°C, washed several times, and eluted with elution buffer according to the manufacturer's protocol (EZ ChIP chromatin immunoprecipitation kit; Millipore). Input and immunoprecipitated chromatin were uncross-linked for 5 to 6 h at 65°C with 12 μL of 5 M NaCl. Associated proteins were degraded by proteinase K. Chromatin were purified using spin columns and eluted in 50 μL of TE buffer. Input and immunoprecipitated chromatin were used for PCR analysis using various *SDD1* promoter-specific primers that were designed to amplify *SDD1* promoter fragments (see Supplemental Table 1 online).

Immunoblots

Total protein was extracted from leaves of 6-week-old plants grown in soilless media under the 12-h photoperiod conditions. Plant tissues were ground in liquid nitrogen and resuspended in extraction buffer (100 mM potassium phosphate buffer, pH 7.8, 1 mM EDTA, 1% Triton X-100, 10% glycerol, and 1 mM DTT). Ten micrograms of total protein from each plant was separated by SDS-PAGE and transferred to a polyvinylidene difluoride membrane (Thermo Fisher Scientific). The membrane was

probed with anti-GFP antibody (Santa Cruz Biotechnology) and detected by the enhanced chemiluminescence Plus protein gel blotting detection system (GE Healthcare).

Genomic DNA Extraction, RNA Extraction, and RT-PCR Analysis

Genomic DNA from the leaves of 3-week-old plants was extracted by the cetyltrimethyl-ammonium bromide (CTAB) method (Richards et al., 2001) and used to determine homozygosity of T-DNA insertion in *gtl1-4* and *gtl1-5* by PCR analysis using GTL1-specific primers and a T-DNA-specific primer (see Supplemental Table 1 online). Total RNA was extracted from shoots of 4-week-old plants or fully expanded leaves of 8-week-old plants using TRIzol (Invitrogen) according to the manufacturer's protocol. One microgram of total RNA was used to synthesize cDNA by the ThermoScript RT-PCR system for first-strand cDNA synthesis (Invitrogen). The same amount of cDNA was used for PCR analysis using primers for *UBC* (26 or 28 cycles) or *ACT2* (28 cycles; internal control), *GTL1* (35, 28, or 25 cycles for Figure 1C, Supplemental Figure 2A online, and Supplemental Figure 2B online, respectively), *Cor15a* (28 cycles), and stomatal development genes including *SDD1* (40 cycles), *MPK3* (28 cycles), and *MPK6* (28 cycles) (see Supplemental Table 1 online).

Statistical Analysis

All bar graphs were analyzed by Student's *t* test for pairwise comparison.

Accession Numbers

Sequence data from this article can be found in the Arabidopsis Genome Initiative or GenBank/EMBL databases under the following accession numbers: *GTL1* (At1g33240; NM_103052) and *SDD1* (At1g04110; NM_100292).

Supplemental Data

The following materials are available in the online version of this article.

- Supplemental Figure 1.** *gtl1* Plants Were Less Wilting in Response to Water Deficit Stress.
- Supplemental Figure 2.** *GTL1* Expression Is Downregulated by Water Stress and Dehydration.
- Supplemental Figure 3.** *gtl1* Plants Have Reduced Light Period Transpiration Rates under Both Well-Watered and Water Deficit Stress Conditions.
- Supplemental Figure 4.** Leaf Morphology and Area of *gtl1* Plants Are Similar to Those of Wild-Type Plants.
- Supplemental Figure 5.** Quantum Efficiency, Dark Respiration, and Light Compensation Point Were Similar Among Genotypes.
- Supplemental Figure 6.** *gtl1* Plants Exhibited Similar Stomatal Aperture, and Transpiration, Germination, and Root Growth Were Similarly Affected by ABA in Wild-Type and *gtl1* Plants.
- Supplemental Figure 7.** *gtl1* Plants Have Increased Trichome Branch Length.
- Supplemental Figure 8.** *GTL1* Does Not Regulate The Expression of *TMM*, *ER*, and *YDA*.
- Supplemental Figure 9.** The N-Terminal DNA Binding Domain of GTL1 Binds to Three Types of GT Elements.
- Supplemental Figure 10.** Stomatal Development Pathways Include a Basal Pathway and a Negative Regulatory Pathway for Fine-Tuning of Stomatal Development in Epidermal Cells.

Supplemental Table 1. Sequence Information Used for Plasmid Construction, RT-PCR, ChIP Analyses, and EMSA.

Supplemental References.

ACKNOWLEDGMENTS

National Science Foundation Award MCB-0424850 and Binational Agricultural Research and Development Awards 103314 supported research in the laboratory of P.M.H. We thank Fernando Alemán for assistance with gene expression analysis and Hua Weng for reviewing this article.

Received August 11, 2010; revised November 11, 2010; accepted November 24, 2010; published December 17, 2010.

REFERENCES

- Ahmed, F.E., Abusam, S.M.A., and Ahmed, E.E.A. (2010). The bases of *Blepharis* sp. adaptation to water-limited environment. *Asian J. Crop Sci.* **2**: 12–19.
- Alon, U. (2007). Network motifs: Theory and experimental approaches. *Nat. Rev. Genet.* **8**: 450–461.
- Bacon, M.A. (2004). *Water Use Efficiency in Plant Biology*. (Oxford, UK: Blackwell Publishing).
- Baker, S.S., Wilhem, K.S., and Thomashow, M.F. (1994). The 5'-region of *Arabidopsis thaliana cor15a* has cis-acting elements that confer cold-, drought-, and ABA-regulated gene expression. *Plant Mol. Biol.* **24**: 701–713.
- Berger, D., and Altmann, T. (2000). A subtilisin-like serine protease involved in the regulation of stomatal density and distribution in *Arabidopsis thaliana*. *Genes Dev.* **14**: 1119–1131.
- Bergmann, D.C. (2004). Integrating signals in stomatal development. *Curr. Opin. Plant Biol.* **7**: 26–32.
- Bergmann, D.C., Lukowitz, W., and Somerville, C.R. (2004). Stomatal development and pattern controlled by a MAPKK kinase. *Science* **304**: 1494–1497.
- Bergmann, D.C., and Sack, F.D. (2007). Stomatal development. *Annu. Rev. Plant Biol.* **58**: 163–181.
- Blum, A. (1996). Crop responses to drought and the interpretation of adaptation. *Plant Growth Regul.* **20**: 135–148.
- Breuer, C., Kawamura, A., Ichikawa, T., Tominaga-Wada, R., Wada, T., Kondou, Y., Muto, S., Matsui, M., and Sugimoto, K. (2009). The trihelix transcription factor GTL1 regulates ploidy-dependent cell growth in the *Arabidopsis* trichome. *Plant Cell* **21**: 2307–2322.
- Brewer, P.B., Howles, P.A., Dorian, K., Griffith, M.E., Ishida, T., Kaplan-Levy, R.N., Kilinc, A., and Smyth, D.R. (2004). *PETAL LOSS*, a trihelix transcription factor gene, regulates perianth architecture in the *Arabidopsis* flower. *Development* **131**: 4035–4045.
- Büßis, D., von Groll, U., Fisahn, J., and Altman, T. (2006). Stomatal aperture can compensate altered stomatal density in *Arabidopsis thaliana* at growth light conditions. *Funct. Plant Biol.* **33**: 1037–1043.
- Casson, S., and Gray, J.E. (2008). Influence of environmental factors on stomatal development. *New Phytol.* **178**: 9–23.
- Casson, S.A., and Hetherington, A.M. (2010). Environmental regulation of stomatal development. *Curr. Opin. Plant Biol.* **13**: 90–95.
- Chaerle, L., Saibo, N., and Van Der Straeten, D. (2005). Tuning the pores: Towards engineering plants for improved water use efficiency. *Trends Biotechnol.* **23**: 308–315.
- Chaves, M.M., Maroco, J.P., and Pereira, J.S. (2003). Understanding plant responses to drought – From genes to the whole plant. *Funct. Plant Biol.* **30**: 239–264.
- Dehesh, K., Bruce, W.B., and Quail, P.H. (1990). A trans-acting factor that binds to a GT-motif in a phytochrome gene promoter. *Science* **250**: 1397–1399.
- Dong, J., and Bergmann, D.C. (2010). Stomatal patterning and development. *Curr. Top. Dev. Biol.* **91**: 267–297.
- Dong, J., MacAlister, C.A., and Bergmann, D.C. (2009). BASL controls asymmetric cell division in *Arabidopsis*. *Cell* **137**: 1320–1330.
- Fan, L.M., Zhang, W., Chen, J.G., Taylor, J.P., Jones, A.M., and Assmann, S.M. (2008). Abscisic acid regulation of guard-cell K⁺ and anion channels in Gbeta- and RGS-deficient *Arabidopsis* lines. *Proc. Natl. Acad. Sci. USA* **105**: 8476–8481.
- Farquhar, G.D., and Sharkey, T. (1982). Stomatal conductance and photosynthesis. *Annu. Rev. Plant Physiol.* **33**: 317–345.
- Green, P.J., Kay, S.A., and Chua, N.H. (1987). Sequence-specific interactions of a pea nuclear factor with light-responsive elements upstream of the *rbcs-3A* gene. *EMBO J.* **6**: 2543–2549.
- Hara, K., Kajita, R., Torii, K.U., Bergmann, D.C., and Kakimoto, T. (2007). The secretory peptide gene *EPF1* enforces the stomatal one-cell-spacing rule. *Genes Dev.* **21**: 1720–1725.
- Hetherington, A.M., and Woodward, F.I. (2003). The role of stomata in sensing and driving environmental change. *Nature* **424**: 901–908.
- Hu, H., Boisson-Dernier, A., Israelsson-Nordström, M., Böhmer, M., Xue, S., Ries, A., Godoski, J., Kuhn, J.M., and Schroeder, J.I. (2010). Carbonic anhydrases are upstream regulators of CO₂-controlled stomatal movements in guard cells. *Nat. Cell Biol.* **12**: 87–93, 1–18.
- Huang, X.Y., Chao, D.Y., Gao, J.P., Zhu, M.Z., Shi, M., and Lin, H.X. (2009). A previously unknown zinc finger protein, DST, regulates drought and salt tolerance in rice via stomatal aperture control. *Genes Dev.* **23**: 1805–1817.
- Hunt, L., Bailey, K.J., and Gray, J.E. (2010). The signalling peptide EPFL9 is a positive regulator of stomatal development. *New Phytol.* **186**: 609–614.
- Hunt, L., and Gray, J.E. (2009). The signaling peptide EPF2 controls asymmetric cell divisions during stomatal development. *Curr. Biol.* **19**: 864–869.
- Impa, S.M., Nadaradjan, S., Boominathan, P., Shashidhar, G., Bindumadhava, H., and Sheshshayee, M.S. (2005). Carbon isotope discrimination accurately reflects variability in WUE measured at a whole plant level in rice. *Crop Sci.* **45**: 2517–2522.
- Jarvis, P.G., and McNaughton, K.G. (1986). Stomatal control of transpiration: Scaling up from leaf to region. *Adv. Ecol. Res.* **15**: 1–49.
- Jin, J.B., et al. (2008). The SUMO E3 ligase, *AtSIZ1*, regulates flowering by controlling a salicylic acid-mediated floral promotion pathway and through affects on *FLC* chromatin structure. *Plant J.* **53**: 530–540.
- Kanaoka, M.M., Pillitteri, L.J., Fujii, H., Yoshida, Y., Bogenschutz, N.L., Takabayashi, J., Zhu, J.K., and Torii, K.U. (2008). *SCREAM/ICE1* and *SCREAM2* specify three cell-state transitional steps leading to *Arabidopsis* stomatal differentiation. *Plant Cell* **20**: 1775–1785.
- Kashiwagi, A., Urabe, I., Kaneko, K., and Yomo, T. (2006). Adaptive response of a gene network to environmental changes by fitness-induced attractor selection. *PLoS ONE* **1**: e49.
- Kim, J.I., et al. (2007). *yucca6*, a dominant mutation in *Arabidopsis*, affects auxin accumulation and auxin-related phenotypes. *Plant Physiol.* **145**: 722–735.
- Kim, T.H., Böhmer, M., Hu, H., Nishimura, N., and Schroeder, J.I. (2010). Guard cell signal transduction network: Advances in understanding abscisic acid, CO₂, and Ca²⁺ signaling. *Annu. Rev. Plant Biol.* **61**: 561–591.
- Kuhn, R.M., Caspar, T., Dehesh, K., and Quail, P.H. (1993). DNA binding factor GT-2 from *Arabidopsis*. *Plant Mol. Biol.* **23**: 337–348.
- Lake, J.A., Quick, W.P., Beerling, D.J., and Woodward, F.I. (2001). Plant development. Signals from mature to new leaves. *Nature* **411**: 154.

- Lambers, H., Chapin, F.S., and Pons, T.L. (1998). *Plant Physiological Ecology*. (New York: Springer).
- Lampard, G.R., Macalister, C.A., and Bergmann, D.C. (2008). *Arabidopsis* stomatal initiation is controlled by MAPK-mediated regulation of the bHLH SPEECHLESS. *Science* **322**: 1113–1116.
- Li, S., Assmann, S.M., and Albert, R. (2006). Predicting essential components of signal transduction networks: A dynamic model of guard cell abscisic acid signaling. *PLoS Biol.* **4**: e312.
- Liu, Q., Kasuga, M., Sakuma, Y., Abe, H., Miura, S., Yamaguchi-Shinozaki, K., and Shinozaki, K. (1998). Two transcription factors, DREB1 and DREB2, with an EREBP/AP2 DNA binding domain separate two cellular signal transduction pathways in drought- and low-temperature-responsive gene expression, respectively, in *Arabidopsis*. *Plant Cell* **10**: 1391–1406.
- MacAlister, C.A., Ohashi-Ito, K., and Bergmann, D.C. (2007). Transcription factor control of asymmetric cell divisions that establish the stomatal lineage. *Nature* **445**: 537–540.
- Masle, J., Gilmore, S.R., and Farquhar, G.D. (2005). The *ERECTA* gene regulates plant transpiration efficiency in *Arabidopsis*. *Nature* **436**: 866–870.
- Morison, J.I.L., Baker, N.R., Mullineaux, P.M., and Davies, W.J. (2008). Improving water use in crop production. *Philos. Trans. R. Soc. Lond. B Biol. Sci.* **363**: 639–658.
- Ni, M., Dehesh, K., Tepperman, J.M., and Quail, P.H. (1996). GT-2: In vivo transcriptional activation activity and definition of novel twin DNA binding domains with reciprocal target sequence selectivity. *Plant Cell* **8**: 1041–1059.
- Nilson, S.E., and Assmann, S.M. (2007). The control of transpiration. Insights from *Arabidopsis*. *Plant Physiol.* **143**: 19–27.
- Nilson, S.E., and Assmann, S.M. (2010). The α -subunit of the *Arabidopsis* heterotrimeric G protein, GPA1, is a regulator of transpiration efficiency. *Plant Physiol.* **152**: 2067–2077.
- Nobel, P.S. (1999). *Physicochemical & Environmental Plant Physiology*. (San Diego, CA: Academic Press).
- Ohashi-Ito, K., and Bergmann, D.C. (2006). *Arabidopsis* FAMA controls the final proliferation/differentiation switch during stomatal development. *Plant Cell* **18**: 2493–2505.
- Perera, I.Y., Hung, C.Y., Moore, C.D., Stevenson-Paulik, J., and Boss, W.F. (2008). Transgenic *Arabidopsis* plants expressing the type 1 inositol 5-phosphatase exhibit increased drought tolerance and altered abscisic acid signaling. *Plant Cell* **20**: 2876–2893.
- Pillitteri, L.J., Sloan, D.B., Bogenschutz, N.L., and Torii, K.U. (2007). Termination of asymmetric cell division and differentiation of stomata. *Nature* **445**: 501–505.
- Richards, E., Reichardt, M., and Rogers, S. (2001). Preparation of genomic DNA from plant tissue. In *Current Protocols in Molecular Biology*, Vol. 1, F.M. Ausubel, R. Brent, R.E. Kingston, D.D. Moore, J. G. Seidman, J.A. Smith, and K. Struhl, eds (New York: John Wiley and Sons), pp. 2.3.1–2.3.7.
- Saez, A., Robert, N., Maktabi, M.H., Schroeder, J.I., Serrano, R., and Rodriguez, P.L. (2006). Enhancement of abscisic acid sensitivity and reduction of water consumption in *Arabidopsis* by combined inactivation of the protein phosphatases type 2C ABI1 and HAB1. *Plant Physiol.* **141**: 1389–1399.
- Shpak, E.D., McAbee, J.M., Pillitteri, L.J., and Torii, K.U. (2005). Stomatal patterning and differentiation by synergistic interactions of receptor kinases. *Science* **309**: 290–293.
- Sinclair, T.R., Tanner, C.B., and Bennett, J.M. (1984). Water use efficiency in crop production. *Bioscience* **34**: 36–40.
- Song, X.J., and Matsuoka, M. (2009). Bar the windows: An optimized strategy to survive drought and salt adversities. *Genes Dev.* **23**: 1709–1713.
- Sugano, S.S., Shimada, T., Imai, Y., Okawa, K., Tamai, A., Mori, M., and Hara-Nishimura, I. (2010). Stomagen positively regulates stomatal density in *Arabidopsis*. *Nature* **463**: 241–244.
- Thattai, M., and van Oudenaarden, A. (2001). Intrinsic noise in gene regulatory networks. *Proc. Natl. Acad. Sci. USA* **98**: 8614–8619.
- Udayakumar, M., Sheshshayee, M.S., Nataraj, K.N., Bindumadhava, H., Devendra, R., Aftab Hussain, I.S., and Prasad, T.G. (1998). Why breeding for water use efficiency has not been successful? An analysis and alternate approach to exploit this trait for crop improvement. *Curr. Sci.* **74**: 994–1000.
- Van den Boogaard, B., Alewijnse, D., Veneklaas, E.J., and Lambers, H. (1997). Growth and water use efficiency of 10 *Triticum aestivum* cultivars at different water availability in relation to allocation of biomass. *Plant Cell Environ.* **20**: 200–210.
- von Groll, U., Berger, D., and Altmann, T. (2002). The subtilisin-like serine protease SDD1 mediates cell-to-cell signaling during *Arabidopsis* stomatal development. *Plant Cell* **14**: 1527–1539.
- Wang, H., Ngwenyama, N., Liu, Y., Walker, J.C., and Zhang, S. (2007). Stomatal development and patterning are regulated by environmentally responsive mitogen-activated protein kinases in *Arabidopsis*. *Plant Cell* **19**: 63–73.
- Xie, Z.M., Zou, H.F., Lei, G., Wei, W., Zhou, Q.Y., Niu, C.F., Liao, Y., Tian, A.G., Ma, B., Zhang, W.K., Zhang, J.S., and Chen, S.Y. (2009). Soybean Trihelix transcription factors GmGT-2A and GmGT-2B improve plant tolerance to abiotic stresses in transgenic *Arabidopsis*. *PLoS ONE* **4**: e6898.
- Xu, Z., and Zhou, G. (2008). Responses of leaf stomatal density to water status and its relationship with photosynthesis in a grass. *J. Exp. Bot.* **59**: 3317–3325.
- Yoo, C.Y., Pence, H.E., Hasegawa, P.M., and Mickelbart, M.V. (2009). Regulation of transpiration to improve crop water use. *Crit. Rev. Plant Sci.* **28**: 410–431.
- Yu, H., Chen, X., Hong, Y.Y., Wang, Y., Xu, P., Ke, S.D., Liu, H.Y., Zhu, J.K., Oliver, D.J., and Xiang, C.B. (2008). Activated expression of an *Arabidopsis* HD-START protein confers drought tolerance with improved root system and reduced stomatal density. *Plant Cell* **20**: 1134–1151.
- Zhang, X., Henriques, R., Lin, S.S., Niu, Q.W., and Chua, N.H. (2006). Agrobacterium-mediated transformation of *Arabidopsis thaliana* using the floral dip method. *Nat. Protoc.* **1**: 641–646.
- Zhou, D.X. (1999). Regulatory mechanism of plant gene transcription by GT-elements and GT-factors. *Trends Plant Sci.* **4**: 210–214.
- Zimmermann, P., Hirsch-Hoffmann, M., Hennig, L., and Gruissem, W. (2004). GENEVESTIGATOR. *Arabidopsis* microarray database and analysis toolbox. *Plant Physiol.* **136**: 2621–2632.